Inhibition of SFRP1 by microRNA-206-3p may be the underlying cause of osteosarcopenia

CHEN YU[1,2*], ZEHUI LU[3*], YONGJUN DU[1,2], YAN LV[1], JUNHUA FANG[1,2], YU ZHAO[4], ZHI PENG[1] and SHENG LU[1]

[1]Department of Orthopedics, The First People's Hospital of Yunnan Province, The Affiliated Hospital of Kunming University of Science and Technology, The Key Laboratory of Digital Orthopedics of Yunnan Provincial, Yunnan Provincial Center for Clinical Medicine in Spinal and Spinal Cord Disorders, Kunming, Yunnan 650000, P.R. China; [2]Graduate School, Kunming Medical University, Kunming, Yunnan 650000, P.R. China; [3]Medicine, Nursing and Health Sciences, Monash University, Clayton, Victoria 3800, Australia; [4]Department of Orthopaedic Surgery, Peking Union Medical College Hospital, Chinese Academy of Medical Sciences and Peking Union Medical College, Beijing 100006, P.R. China

Received August 18, 2024; Accepted November 27, 2024

DOI: 10.3892/br.2025.1981

Abstract. Osteosarcopenia is characterized by a simultaneous decrease in bone mass and muscle quality. Thus, determining the common pathogenesis between osteoporosis and sarcopenia may aid in identifying a solution. Secreted frizzled-related protein 1 (SFRP1), a Wnt/β-catenin pathway inhibitor, reportedly decreases during the osteogenesis process and is increased in osteoporosis and sarcopenia mice models. As microRNAs (miRNAs/miRs) can regulate the expression of multiple proteins, the present study aimed to determine if miR-206-3p can promote the nuclear translocation of β-catenin by inhibiting SFRP1 during both osteogenesis and myogenesis. Transcriptome sequencing revealed that SFRP1 was markedly upregulated in the BMSCs derived from ovariectomized mice. *In vitro* induction of osteogenesis confirmed that SFRP1 negatively regulated osteogenesis. A luciferase reporter assay confirmed that miR-206-3p downregulated SFRP1 by directly binding to the 3' untranslated region. Subsequently, the BMSC and L6 cells were transfected with an miR-206-3p inhibitor or a corresponding negative control. Immunoblotting was performed to assess the relative expression levels of SFRP1 and Wnt/β-catenin signaling. The mRNA levels of SFRP1, osteogenesis-related molecules and myogenesis-related molecules were also detected by quantitative real-time PCR. The miR-206-3p inhibitor reduced the expression of osteogenesis- and myogenesis-related molecules and inactivated the Wnt/β-catenin signaling by releasing SFRP1. In conclusion, miR-206-3p downregulated SFRP1 and activated Wnt/β-catenin signaling to promote osteogenesis and myogenesis. Thus, miR-206-3p may be an important therapeutic target in osteosarcopenia. The present study aimed to uncover the genes and mechanisms that co-regulate muscle and bone. SFRP1, a known regulator of osteoporosis, was examined by analyzing its upstream regulatory microRNA and validating its molecular role. The diagnostic and therapeutic potential of miR-206-3p for osteomyopenia was evaluated by first focusing on osteoporosis and then validating findings with myofibroblasts. These data suggested that miR-206-3p can serve as a therapeutic target for osteomyopenia by inhibiting SFRP1, thereby activating the Wnt/β-catenin signaling pathway and promoting both osteogenesis and myogenesis.

Correspondence to: Dr Zhi Peng or Professor Sheng Lu, Department of Orthopedics, The First People's Hospital of Yunnan Province, The Affiliated Hospital of Kunming University of Science and Technology, The Key Laboratory of Digital Orthopedics of Yunnan Provincial, Yunnan Provincial Center for Clinical Medicine in Spinal and Spinal Cord Disorders, 157 Jinbi Road, Kunming, Yunnan 650000, P.R. China
E-mail: zhiandpeng@126.com
E-mail: drlusheng@163.com

*Contributed equally

Key words: osteogenesis, myogenesis, secreted frizzled related protein 1, miR-206-3p, WNT/β-catenin pathway

Introduction

The pathogeneses of osteoporosis and sarcopenia, the two most common diseases encountered in older adults, are closely related to age (1). Osteoporosis refers to the deterioration of bone density and microarchitecture (2), whereas sarcopenia refers to defects in muscle quantity, quality and function (3). Numerous studies have demonstrated that muscles and bones are spatially and metabolically connected (4). Furthermore, individuals with sarcopenia are five times more likely to develop osteoporosis than healthy individuals and vice versa (5). Therefore, some studies have termed the coexistence of osteoporosis and sarcopenia as osteosarcopenia (6,7). The presence of OS leads to more fractures, frailty, hospitalization, disability and mortality than osteoporosis or sarcopenia alone (6).

Muscle and bone share a common origin of mesenchymal precursors (8). Furthermore, several molecular mechanisms regulate both muscles and bones (9). Thus, finding the common molecule that affects the progress of osteogenesis and myogenesis could help determine the pathogenesis of osteosarcopenia. Bone marrow mesenchymal stem cells (BMSC) are pluripotent stem cells with trilineage differentiation abilities, which include osteogenesis, lipogenesis and chondrogenesis (10,11). L6 is a myoblast strain isolated from the skeletal muscle of rats that be used to study myogenesis. Secreted frizzled-related protein 1 (SFRP1) is an antagonist of the Wnt signaling pathway that binds to Wnt proteins and prevents it from interacting with their cell surface receptors. This helps regulate the balance between cell proliferation and differentiation, which is essential for normal development and tissue homeostasis. Dysregulation of SFRP1 has been implicated in various human diseases, including cancer, fibrosis and degenerative disorders.

SFRP1, which modulates the Wnt signaling pathway, plays a significant role in bone and muscle development, homeostasis and regeneration. SFRP1 plays a role in the regulation of osteoblast differentiation by inhibiting the Wnt signaling pathway. Thus, a decrease in SFRP1 expression can increase bone formation and reduce bone resorption, whereas an increase in SFRP1 expression can decrease bone mass and increase susceptibility to fractures. SFRP1 also plays a role in myogenesis, the process of muscle tissue formation and post-injury muscle regeneration. SFRP1 promotes the activation and differentiation of muscle satellite cells, which are responsible for muscle repair and growth. Additionally, SFRP1 inhibition may have a role in preventing muscle atrophy, which is the loss of muscle mass due to various factors such as aging or diseases. Thus, SFRP1 may be a potential therapeutic target to prevent muscle atrophy.

Although these findings suggested that SFRP1 may be an essential molecule in osteosarcopenia, its upstream regulator remains unknown. microRNAs (miRNAs/miRs) are small non-coding RNA molecules that play a crucial role in regulating gene expression at the post-transcriptional level. They can modulate the stability and translation of messenger RNA (mRNA) molecules to control protein synthesis and cellular functions.

By binding to the 3'UTR of target mRNA, they enable degradation or inhibition of translation. Additionally, they participate in complex life processes such as cell proliferation, differentiation, apoptosis and carcinogenesis, which are closely related to the occurrence, development, prognosis, diagnosis and treatment of several diseases (12,13). miRNAs are involved in the proliferation and differentiation of bones or muscles (14-16). For example, miR-34a-5p promotes osteogenic differentiation by targeting HDAC1 (17), miR-29a-3p promotes proliferation and inhibits osteogenic differentiation by targeting FOXO3 (18), miR-130b inhibits proliferation and promotes myoblast differentiation by targeting Sp1 (19) and miR-452 promotes proliferation and inhibits myoblast differentiation by targeting ANGPT1 (20). However, only a few studies have evaluated miRNAs that regulate both bone and muscle actions through a single pathway.

Muscle and bone share a common origin and are regulated by several molecular mechanisms (9). Osteoblasts and myoblasts originate from the same mesenchymal stem cells (8). Among these, bone marrow mesenchymal stem cells (BMSC)s are currently being studied (10). In osteoporosis, the osteogenic capacity of BMSC is diminished, which decreases bone formation (11).

The present study extracted bone marrow stem cells from osteoporotic and control rats for transcriptome sequencing to identify the differential gene SFRP1. The results indicated that miR-206-3p might target SFRP1. miR-1, miR-133 and miR-206 are known muscle-specific miRNAs that play an important role in muscle growth and development (21). Therefore, the regulatory roles of miR-206-3p was assessed in BMSC and myogenic cells. The results demonstrated that miR-206-3p targets SFRP1 through the Wnt/β-catenin signaling pathway, which in turn affects muscle and bone differentiation.

Materials and methods

Animals. The experimental animal study protocol was approved by the Animal Care and Use Committee of the Kunming Medical University, Kunming, China (approval no. kmmu20230916). All animal experiments and handling were performed in accordance with the Guide for the Care and Use of Laboratory Animals published by the National Institutes of Health [NIH Publication No. 8523, revised 1985 (22)]. A total of six-week-old, healthy, female Sprague-Dawley rats, each weighing 250-300 g, free of specific pathogens, were purchased from the Department of Laboratory Animal Science, Kunming Medical University. All animals were maintained under a standard 12-h light/dark cycle with free access to food and water. Environmental conditions were maintained with relative humidity ranging from 30-60% and a temperature of 23±2˚C. After adaptive feeding, the rats were ovariectomized (OVX group) or subjected to a sham surgery (sham group; n=3 per group). Subsequently, the rats were fed for 3 months and euthanized. Subsequently, the rats were fed for 3 months and sacrificed. Sacrifice was by intraperitoneal injection of excessive sodium pentobarbital (100 mg/kg).

Ovariectomization. Rats were anesthetized intraperitoneally with 3% sodium pentobarbital (30 mg/kg) and ovariectomy (OVX) was performed under anesthesia. After making incisions on both sides of the abdominal midline, the proximal end of each fallopian tube was ligated and the ovaries were isolated. After bilateral ovaries were excised with scissors, the wound was sutured.

Microcomputed tomography scanning. After the rats were euthanized, the femurs were isolated and scanned using micro-computed tomography (CT). The distal femur was scanned to determine the trabecular bone volume/tissue volume ratio (BV/TV), bone mineral density (BMD) and trabecular thickness (TbTh).

Hematoxylin and eosin staining. The rat femurs were fixed with 4% paraformaldehyde for 24 h. Thereafter, the specimens were soaked in 70% ethanol for 3 days at 4˚C and the liquid was changed every day. Subsequently, the specimens were

embedded in paraffin and cut into 5-μm sections. Finally, the sections were deparaffinized, rehydrated and stained with hematoxylin and eosin. The sections were stained 10 min at room temperature and observed using a light microscope (magnification, x20).

Von Kossa staining. The rat femurs were fixed with 4% paraformaldehyde for 24 h then immersed in 70% ethanol with daily solution changes for 3 days and stored at 4˚C. All subsequent procedures were performed at 4˚C whenever possible. Thereafter, embedding and sectioning were performed to obtain 5 μm thick hard tissue sections. The sections were stained using Von Kossa solution (Beijing Solarbio Science & Technology Co., Ltd.) following the manufacturer's instructions: Von Kossa silver solution was added dripwise to the sections which were then irradiated with strong light for 15-60 min at room temperature before being washed with distilled water for 1 min at room temperature. After sealing, the sections were observed under a light microscope (magnification, x20).

Toluidine blue O solution. After being fixed with 4% paraformaldehyde for 24 h, the rat femurs were soaked in 70% ethanol for 3 days at 4˚C. The ethanol was changed every day. Thereafter, the femur was sectioned at 5 μm and stained with toluidine blue solution (Beijing Solarbio Science & Technology Co., Ltd.). The sections were stained with 1% toluidine blue O solution for 10 min at room temperature and observed using a light microscope (magnification x20).

Tartrate-resistant acidic phosphatase staining. After being fixed with 4% paraformaldehyde for 24 h, the rats femurs were soaked in 70% ethanol for 3 days at 4˚C. The ethanol was changed every day. Thereafter, the femur was sectioned at 5 μm and stained using tartrate-resistant acidic phosphatase (TRAP; Wuhan Servicebio Technology Co., Ltd.). The sections were reacted with tartrate-resistant acidic phosphatase working solution for 20 min at 37˚C in the dark and observed using a light microscope (magnification x20).

BMSC isolation and culture. BMSCs were isolated from the bone marrow aspirate of the rat femurs. In the OVX group, the BMSCs were isolated 3 months after OVX. After being euthanized, the rats femurs were dissected out aseptically and the external soft tissue was discarded. A 20-gauge needle was used to prepare the cell suspension by repeatedly flushing the bone marrow lumen with minimum essential medium (Gibco; Thermo Fisher Scientific, Inc.) containing 1% penicillin/streptomycin (Gibco; Thermo Fisher Scientific, Inc.). The cells were inoculated into cell culture flasks and subsequently inoculated in an α-minimal essential medium supplemented with 10% fetal bovine serum (FBS; Gibco; Thermo Fisher Scientific, Inc.) and 1% penicillin/streptomycin at 37˚C in a humidified atmosphere of 5% CO_2.

Flow cytometry identification of BMSC. Third-generation BMSCs were digested with TrypLE (Gibco; Thermo Fisher Scientific, Inc.) and the cells were resuspended in a complete medium to produce single-cell suspensions containing $5x10^5$-$1x10^6$ cells/ml. Thereafter, the cells were washed twice with PBS containing 1% bovine serum albumin (1% BSA/PBS; Beijing Solarbio Science & Technology Co., Ltd.). Thereafter, the cells were resuspended in 1% BSA/PBS before being transplanted into Eppendorf tubes. CD29 (Invitrogen; Thermo Fisher Scientific, Inc.; cat. no. 2282645), CD44 (Invitrogen; Thermo Fisher Scientific, Inc.; cat. no. 2252597), CD45 (Invitrogen; Thermo Fisher Scientific, Inc.; cat. no. 2265339) and CD90 (Invitrogen; Thermo Fisher Scientific, Inc.; cat. no. 2227596) cells and the antibody compensation beads were added to the Eppendorf tubes according to the manufacturer's instructions. The tubes were incubated at 4˚C for 60 min. Thereafter, the cells were washed with 1%BSA/PBS twice at 4˚C before being resuspended. Finally, the cells were analyzed by flow cytometry (BD FACSCelesta™), and analyzed using FlowJov10.6.2 (FlowJo LLC).

Trilineage differentiation and staining of BMSCs. BMSCs were placed in osteogenic, lipogenic and chondrogenic induction media to induce differentiation. The osteogenic, lipogenic and chondrogenic differentiation of BMSCs was determined by staining with alizarin red, oil red O and Alcian blue, respectively. For osteogenic differentiation, alizarin red staining working solution stained cells for 6 min at room temperature. For adipogenic differentiation, oil red O staining working solution was used to stain cells for 30 min at room temperature. For chondrogenic differentiation, Alcian blue staining working solution was stained at 37˚C for 1 h.

Transcriptome sequencing of BMSCs. The BMSCs obtained from the OVX and Sham groups were cultured up to P3 generation and four samples containing 5 million cells each were obtained from each group. To extract the total RNA from the cells, 1 ml of TRIzol® (Thermo Fisher Scientific, Inc.) was added to each sample and the concentration and purity of the extracted RNA were detected using NanoDrop 2000 (NanoDrop Technologies; Thermo Fisher Scientific, Inc.). After the RNA quality control had reached the standard, the ribosomal RNA was removed and fragmented into small segments of approximately 200 bp. Reverse transcription is then performed to generate cDNA. The double-stranded cDNA structure has sticky ends, which are converted to blunt ends by adding an End Repair Mix. Subsequently, a single A base is added to the 3' end to facilitate the ligation of a Y-shaped adapter, forming the adapter-ligated product. The product is then purified and subjected to size selection. The selected fragments are amplified by PCR, and the final library is purified. The library is sequenced using the Illumina NovaSeq 6000 platform (Illumina, Inc.).

L6 cell culture and myogenic differentiation. L6 cells were obtained from the Fan Wenxing Research Group of the First Affiliated Hospital of Kunming Medical University. The L6 cells were inoculated in a high-glucose Dulbecco's modified Eagle's medium (DMEM; Gibco; Thermo Fisher Scientific, Inc.) supplemented with 10% FBS and 1% penicillin-streptomycin. These were then incubated in a constant-temperature cell incubator at 37˚C and 5% CO_2. When the L6 cells had reached 60% confluence, the growth medium was aspirated and the cells were washed twice with PBS. Thereafter, a medium that induced myogenic differentiation [DMEM supplemented

Table I. Primers.

Gene symbol	Forward	Reverse
SFRP1	TACTGGCCCGAGATGCTCAA	TACTGGCCCGAGATGCTCAA
GAPDH	CAGGTTGTCTCCTGTGACTT	TTATGGGGTCTGGGATGGAA
U6	TGGAACGCTTCACGAATTTGCG	GGAACGATACAGAGAAGATTAGC
miR-206-3p	CGTGGAATGTAAGGAAGTGTGTGG	

SFRP1, secreted frizzled-related protein 1; miR, microRNA.

with 2% horse serum (Gibco; Thermo Fisher Scientific, Inc.)] was added. The differentiation medium was replaced daily.

Reverse transcription-quantitative (RT-q) PCR. Total RNA was extracted from cells ($1x10^6$ cells/ml) using TRIzol® (Thermo Fisher Scientific, Inc.) following the manufacturer's protocol. RNA (1 μg per sample) was then reverse-transcribed into cDNA using a reverse transcription kit (RR036A, Takara Biotechnology Co., Ltd.). qPCR was performed with the TB Green Premix Ex Taq II kit (RR820A, Takara Biotechnology Co., Ltd.) on a QuantStudio3 Real-Time PCR System (Applied Biosystems; Thermo Fisher Scientific, Inc.). All procedures were performed according to the manufacturer's instructions. The PCR amplification conditions were 95˚C for 30 sec (initial denaturation), next 40 cycles of 95˚C for 5 sec, and 60˚C for 34 sec, then 95˚C for 5 sec and 60˚C for 60 sec (dissociation), then cooled to 37˚C. Relative gene expression was determined using the $2^{-\Delta\Delta Cq}$ (23) method and normalized to GAPDH mRNA expression. All mRNA primers (Table I) were synthesized by Sangon Biotech Co., Ltd. To detect miRNA expression, total miRNA was extracted from the cells using RNAiso for small RNA (9753A, Takara Biotechnology Co., Ltd.). The miRNAs were reverse transcribed using the Mir-X miRNA First-Strand Synthesis kit (638313, Takara Biotechnology Co., Ltd.). RT-qPCR was performed using the miRNA tailing reaction. The relative transcription levels of miRNA were normalized to that of U6 RNA. All miRNA primers (Table I) were synthesized by Sangon Biotech Co., Ltd.

Western blotting. RIPA lysate (Beijing Solarbio Science & Technology Co., Ltd.) was used to lyse the cells and extract the proteins. A total of 20 μg (as measured by the BCA protein assay kit) of the protein sample was electrophoresed on a 10% sodium dodecyl sulfate-polyacrylamide gel. The isolated proteins were transferred to a polyvinylidene difluoride membrane by wet transfer. The PVDF membranes were blocked at room temperature in 5% skimmed milk for 2 h and incubated overnight with the primary antibody at 4˚C. Subsequently, the PVDF membranes were incubated with horseradish peroxide-coupled secondary antibodies for 2 h at 25˚C. The results were visualized using an enhanced chemiluminescence solution (MilliporeSigma) after washing the membranes. The protein bands were quantified using ImageJ v1.8.0 (National Institutes of Health). The antibody and dilution ratios were as follows: GAPDH, 1:50,000, Proteintech Group, Inc., cat. no. 10494-1-AP; osteopontin (OPN), 1:4,000, Proteintech Group, Inc., cat. no. 22952-1-AP; osteocalcin (OCN), 1:1,000, Proteintech Group, Inc., cat. no. 23418-1-AP; SFRP1, 1:1,000, Bioss, bs-1303R; lycogen synthase kinase 3 beta (GSK3β), 1:5,000, Proteintech Group, Inc., cat. no. 82061-1-RR; α-tubulin, 1:5,000, Proteintech Group, Inc., cat. no. 11224-1-AP; HRP-conjugated Goat Anti-Rabbit lgG(H+L), 1:10,000, Proteintech Group, Inc., cat. no. SA 00001-2; and HRP-conjugated Goat Anti-Mouse IgG(H+L), 1:10,000, Proteintech Group, Inc., cat. no. SA 00001-1. GAPDH was used as an internal reference protein in Fig. 5, while α-tubulin was used in Figs. 2-4.

Plasmid transfection. The miR-206-3p inhibitor and its negative control (miR-NTC) were purchased from Shanghai GeneChem Co., Ltd. The cells were transfected with Lipofectamine® 3000 (Invitrogen; Thermo Fisher Scientific, Inc.), according to the manufacturer's instructions. The transfected nucleic acid concentration was 50 nm. Transfection was performed for 20 min at room temperature to form complexes and then cells were incubated at 37˚C in a 5% CO_2 incubator. The transfected cells were subjected to follow-up experiments 24-48 h after transfection. Negative control sequence: TTC TCCGAACGTGTCACGT.

Dual-luciferase reporter assay. A total of 293 cells were cultured to a density of $2x10^4$ cells/well in 96-well culture plates. The cells were transfected with dual-luciferase reporter (DLR) construct p1 (0.2 μg) or co-transfected with DLR construct p2 (0.2 μg) and the internal control vector pRL-TK, pRL-SV40, or pRL-CMV (Promega Corporation) at a ratio of 20:1 using Lipofectamine® 2000 (Invitrogen; Thermo Fisher Scientific, Inc.). At 5 h following transfection, the transfection medium was removed and replenished with a medium containing 6 μM of curcumin (MilliporeSigma) solubilized in 100% dimethylsulfoxide (MilliporeSigma). At 48 h following transfection, luciferase activity was measured using a DLR assay (Promega Corporation). Renilla luciferase activity was normalized to firefly luciferase activity in cells transfected with the DLR construct p1 and firefly luciferase activity was normalized to Renilla luciferase activity in cells co-transfected with DLR construct p2 and the control vector.

TargetScan. The candidate target miRNA of SFRP1 was predicted using TargetScan (http://www.targetscan.org/).

Statistical analysis. Experimental data were expressed as means ± standard deviation. Statistical analysis was performed using SPSS (version 19.0; IBM Corp.). Data were analyzed

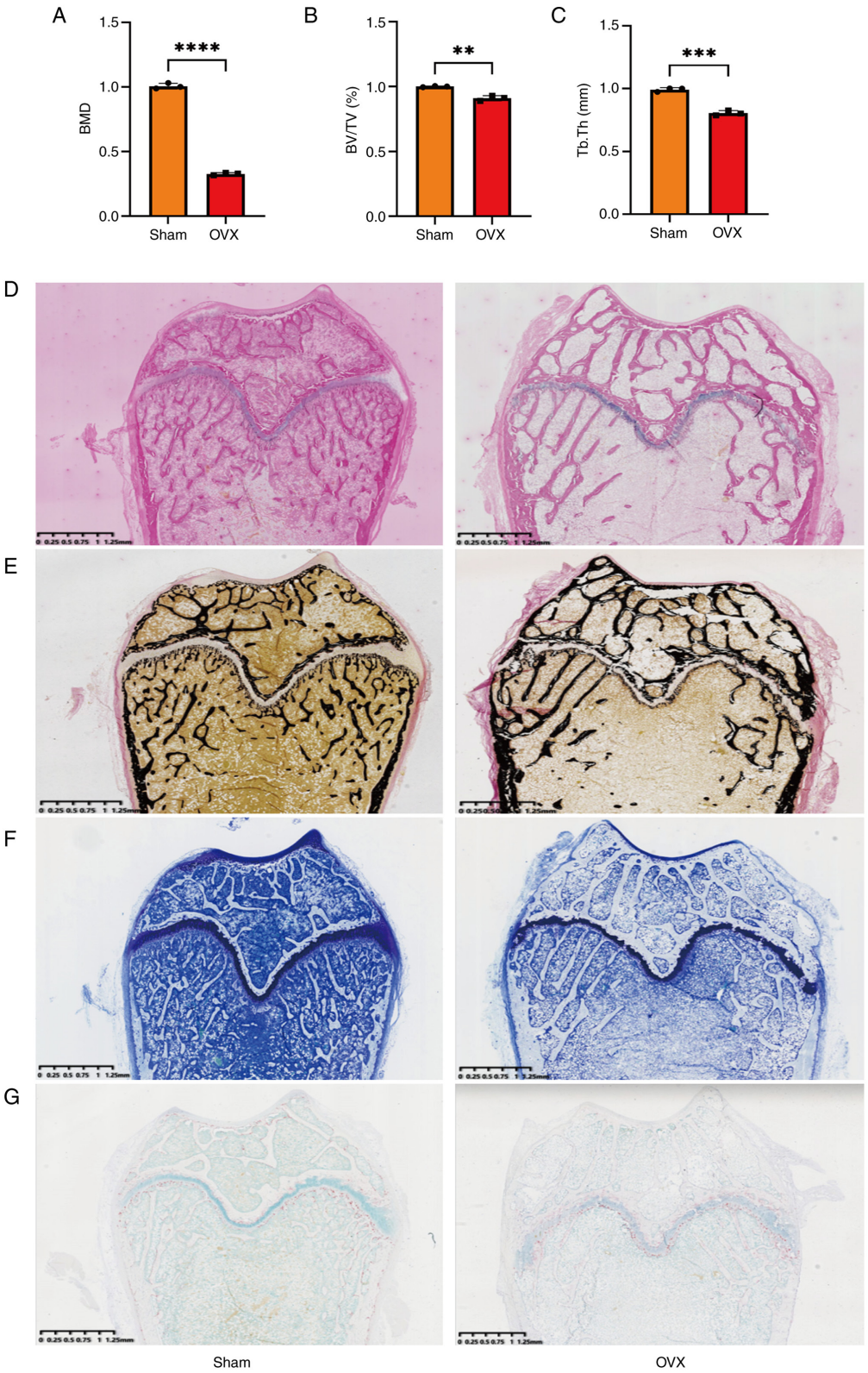

Figure 1. Quantitative analysis of micro-CT data and histological staining results. Quantitative analysis of (A) BMD, (B) BV/TV and (C) TbTh. Results of (D) H&E, (E) Von Kossa, (F) toluidine blue and (G) TRAP staining. Data were analyzed using Student's t-test (n=3). **P<0.01, ***P<0.001, ****P<0.0001. CT, computed tomography; BMD, bone mineral density; BV/TV, bone volume/tissue volume ratio; TbTh, trabecular thickness; H&E, hematoxylin and eosin; TRAP, tartrate-resistant acidic phosphatase.

using Welch and Brown-Forsythe versions of one-way ANOVA or Student's t-test and compared using the χ^2 test. All experiments were repeated at least three times. P<0.05 was considered to indicate a statistically significant difference.

Results

Establishment and identification of osteoporosis model in the OVX group. An osteoporosis rat model was established

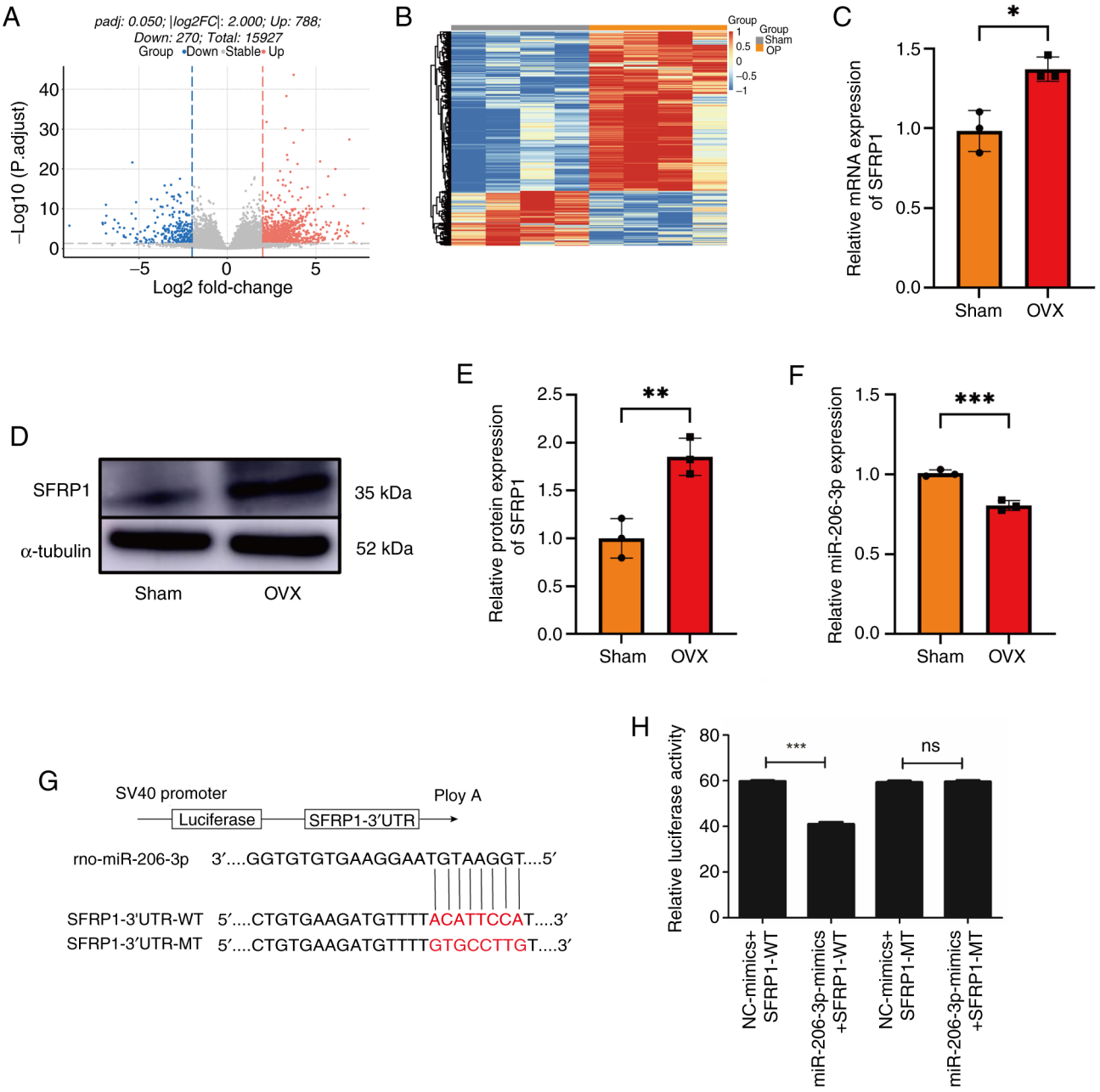

Figure 2. SFRP1 and miR-206-3p are expressed in the BMSCs of the OVX and Sham groups. mRNA differential analysis in the form a (A) volcano plot and (B) clustering heatmap. (C) quantitative PCR revealed in BMSCs that compared with the Sham group, the OVX group demonstrated an increase in the expression of SFRP1. GAPDH was used as an internal reference in the PCR experiments. (D) Western blotting results and (E) quantification in BMSCs. Compared with the Sham group, the OVX group demonstrated an increase in the expression of SFRP1. Gel blots cropped from different parts of the gel and separated by black lines are presented. α-tubulin was used as an internal reference in this experiment. (F) PCR revealed that compared with the Sham group, the OVX group demonstrated an increase in the expression of miR-206-3p. U6 was used as an internal reference in the PCR experiments. (G,H) Dual-luciferase reporter assay demonstrated that miR-206-3p could bind to SFRP1. Data were analyzed using Student's t-test (n=3). *P<0.05, **P<0.01, ***P<0.001. SFRP1, secreted frizzled-related protein 1; miR, microRNA; BMSCs, bone marrow mesenchymal stem cells; OVX, ovariectomized.

by ovariectomy and the degree of osteoporosis was evaluated using histological staining. Quantitative analysis of micro-CT data demonstrated that BMD, BV/TV and TbTh were lower in the OVX group than in the Sham group (Figs. 1A-C and S1). Furthermore, immunohistochemical staining of the rat femurs demonstrated an imbalance in bone metabolism in the OVX group. The resultant reduction in bone mineral density and damage to bone microarchitecture confirmed the presence of osteoporosis in the OVX group (Fig. 1D-G).

Isolation, culture, identification and three-line differentiation of the BMSCs from the rat bone marrow. The differentiation of the extracted BMSCs into osteogenic, lipogenic and chondrogenic cells was confirmed using alizarin red, oil red O and Alcian blue staining, respectively (Fig. S2). Flow cytometry demonstrated that BMSCs displaying $CD29^{+}$, $CD44^{+}$, $CD45^{-}$ and $CD90^{+}$ had a purity of >98.6% (Fig. S3). This indicates that the cells extracted using the method of the present study were rat BMSCs. Western blotting demonstrated that the expression of OPN and OCN were significantly lower in the

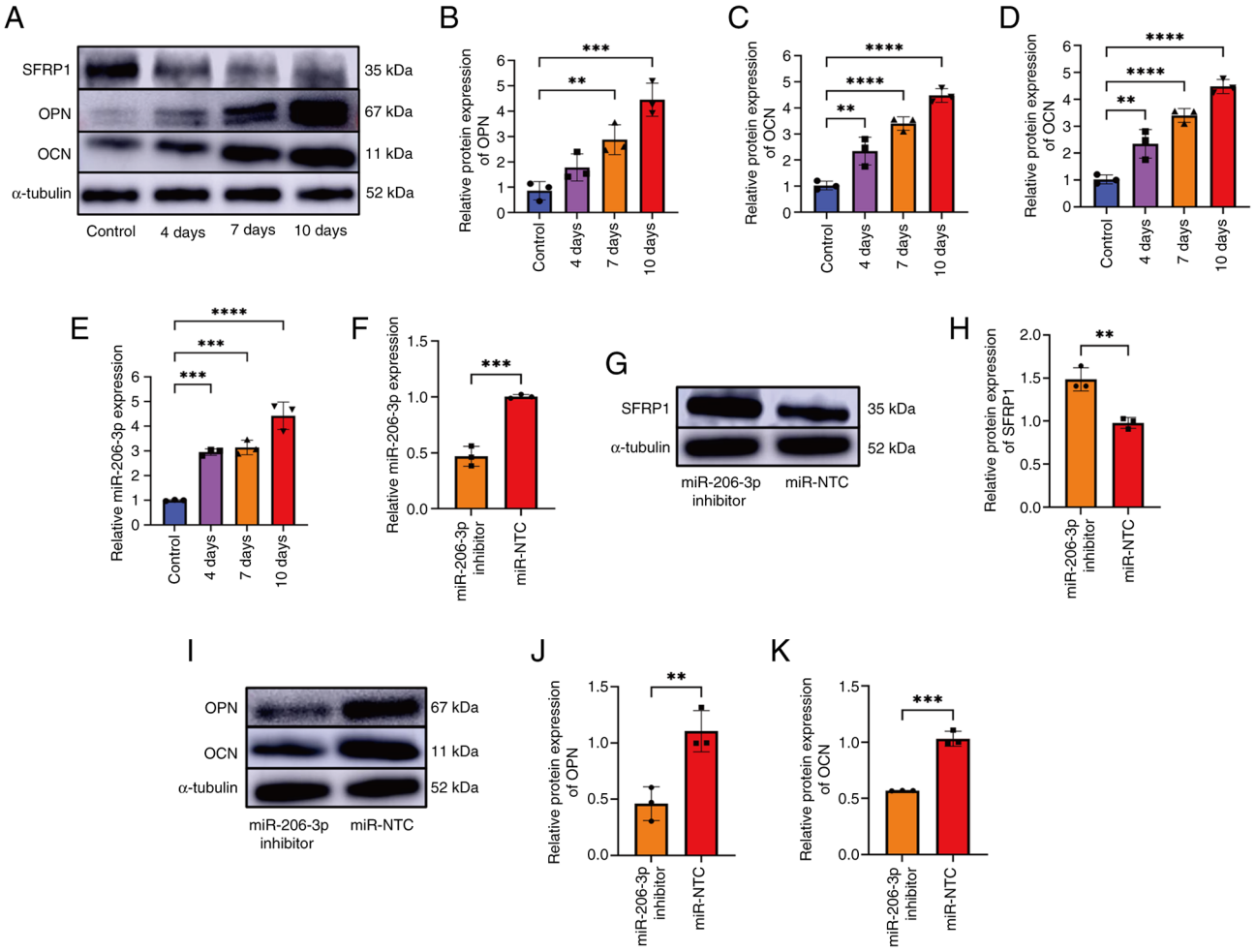

Figure 3. Detection of the osteogenic ability of miR-206-3p inhibitor-transfected BMSCs. (A-D) Expression levels of SFRP1, OPN and OCN at 0, 4, 7 and 10 days during osteogenic differentiation. (E) PCR revealed that the expression of miR-206-3p was upregulated at 0, 4, 7 and 10 days, respectively. (F) PCR revealed that compared with the miR-NTC group, the miR-206-3p inhibitor group demonstrated a reduction in the expression of miR-206-3p. U6 was used as an internal reference in PCR. (G and H) The expression level of SFRP1 increased following the silencing of miR-206-3p. (I-K) The expression of OPN and OCN were detected using western blotting. The presented gel blots have been cropped from different parts of the gel and are separated with black lines. Data were analyzed using the Welch and Brown-Forsy versions of one-way ANOVA (B-E) or Student's t-test (F-K) and compared using the χ^2 test. **P<0.01, ***P<0.001, ****P<0.0001. miR, microRNA; BMSCs, bone marrow mesenchymal stem cells; SFRP1, secreted frizzled-related protein 1; OPN, osteopontin; OCN, osteocalcin; NTC, negative control.

BMSC of the OVX group than in the BMSC of the Sham group (Fig. S4). This indicated that the osteogenic differentiation ability of BMSCs in the OVX group was lower than that in the Sham group.

SFRP1 increases in the OVX group's BMSCs and decreases during osteogenesis. RNA sequencing revealed that, compared with the Sham group, 788 mRNAs were upregulated and 270 mRNAs were downregulated in the OVX group (Table SI). Fig. 2A and B shows the mRNA differential analysis volcano plot and clustering heatmap. Among the markedly upregulated mRNA, SFRP1 negatively regulates osteoblasts and osteoblast functions and it plays an important role in maintaining bone stability. Therefore, SFRP1 was selected as the research object. Results of the RT-qPCR and western blotting for the detection of SFRP1 expression were consistent with those of RNA sequencing (Fig. 2C-E). TargetScan (http://www.targetscan.org/) predicted that miR-206-3p directly targeted the 3'UTR region of SFRP1 (Fig. S5). RT-qPCR revealed that miR-206-3p expression was downregulated in the BMSCs of the OVX group and the expression of miR-206-3p was negatively associated with that of SFRP1 (Fig. 2F). DLR assay was performed to detect the binding sites between miR-206-3p and SFRP1 (Fig. 2G and H). These findings indicated that miR-206-3p may directly target SFRP1 mRNA.

miR-206-3p regulates the osteogenic differentiation of BMSCs by targeting SFRP1. The expression levels of miR-206-3p during osteogenic differentiation after transfection were measured at 4, 7 and 10 days (Fig. 3A-E). The expression level of miR-206-3p increased markedly during osteogenic differentiation. To explore the function of miR-206-3p during osteogenic differentiation of the BMSCs, the BMSCs were transfected with an miR-206-3p inhibitor or a negative control (miR-NTC). Subsequently, RT-qPCR demonstrated that the expression of miR-206-3p was significantly inhibited following silencing (Fig. 3F). Furthermore, the SFRP1 expression increased after the miR-206-3p was silenced (Fig. 3G and H). After the transfected BMSCs were induced to undergo osteogenic differentiation for 7 days, osteoblast-specific markers (OPN and OCN) were

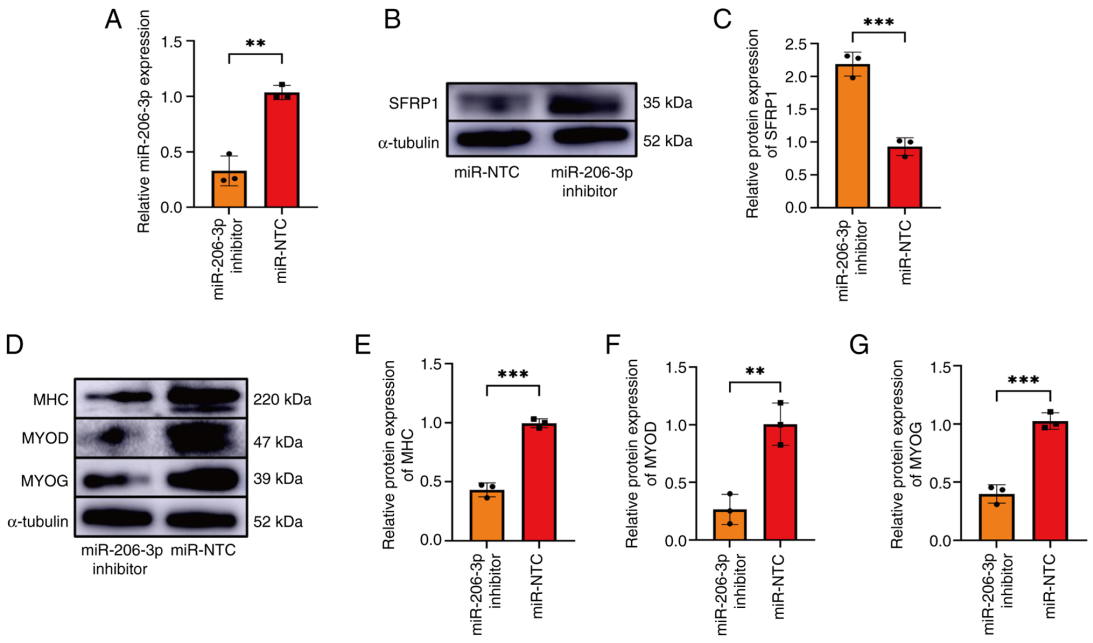

Figure 4. Detection of the myogenic differentiation ability of miR-206-3p inhibitor-transfected L6 cells. (A) PCR revealed that compared with the control group, the miR-206-3p inhibitor group exhibited a significant inhibition of miR-206-3p expression. (B and C) SFRP1 expression increased in the miR-206-3p inhibition group. (D-G) Western blotting revealed a decrease in the MYOD, MYOG and MHC expression levels in the miR-206-3p inhibition group. The presented gel blots have been cropped from different parts of the gel and are separated with black lines. Data were analyzed using Student's t-test (n=3). **P<0.01, ***P<0.001. miR, microRNA; SFRP1, secreted frizzled-related protein 1; MyoD, myogenic differentiation 1; MYOG , myogenin; myosin heavy chain; NTC, negative control.

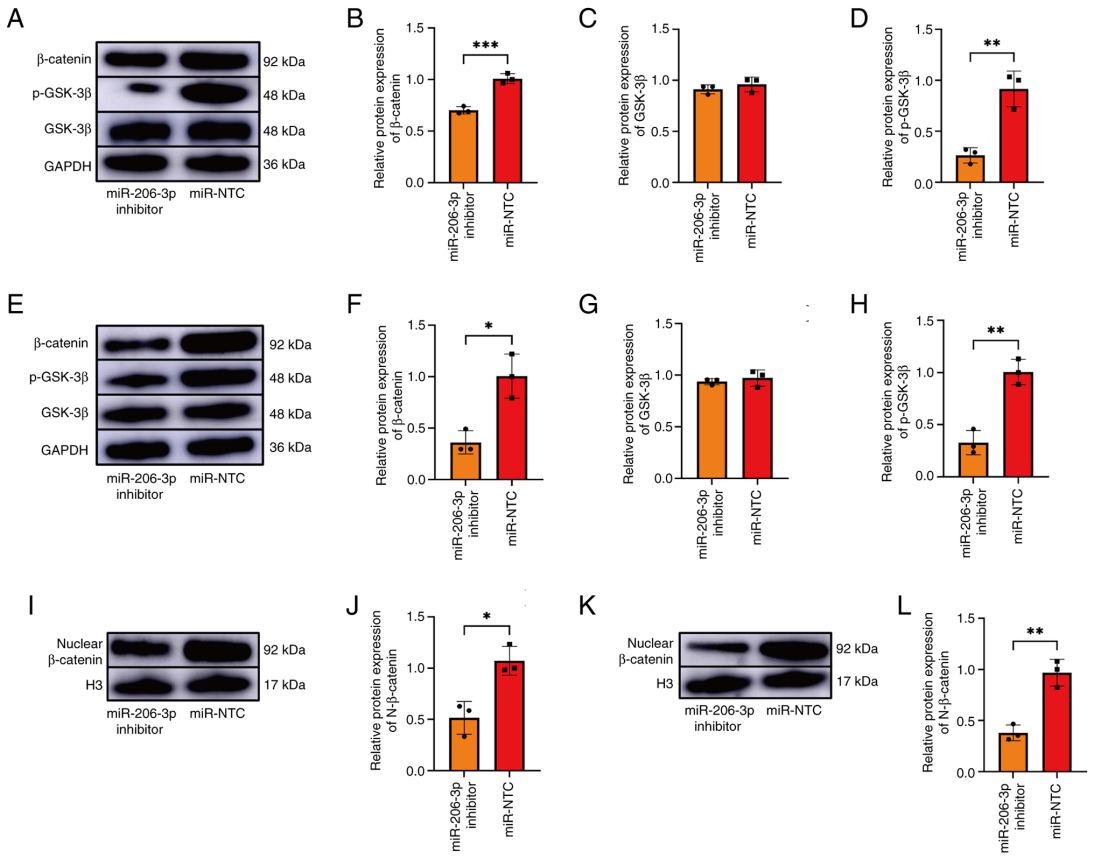

Figure 5. Expression of GSK-3β, p-GSK-3β, β-catenin and nuclear β-catenin in the transfected BMSCs and L6 cells. (A-D) The expression of GSK-3β, p-GSK-3β, β-catenin, SFRP1 were detected by western blotting in the transfected group of BMSC. (E-H) The expression of GSK-3β, p-GSK-3β, β-catenin and SFRP1 in the transfected L6 cells was detected by western blotting. (I and J) The expression of nuclear β-catenin in the transfected BMSCs. (K and L) The expression of nuclear β-catenin in the transfected L6 cells. The presented gel blots have been cropped from different parts of the gel and are separated with black lines. Data were analyzed using Student's t-test (n=3). *P<0.05, **P<0.01, ***P<0.001. GSK, glycogen synthase kinase; p-, phosphorylated; BMSCs, bone marrow mesenchymal stem cells; SFRP1, secreted frizzled-related protein 1; NTC, negative control.

detected by western blotting. The results demonstrated that the osteogenic ability of BMSC in the miR-206-3p inhibition group was weaker compared with the control group (Fig. 3I-K).

miR-206-3p regulates the myogenic differentiation of L6 cells by targeting SFRP1. To investigate the role of miR-206-3p in myoblast differentiation, L6 cells were transfected with an miR-206-3p inhibitor or miR-NTC at 70% density. Thereafter, RT-qPCR revealed that compared with the control group, miR-206-3p expression was significantly inhibited in the miR-206-3p inhibitor group (Fig. 4A). Furthermore, an increase in SFRP1 expression in the miR-206-3p inhibition group was detected (Fig. 4B and C). Following the induction of myogenic differentiation in the transfected L6 cells, the expression of myogenic differentiation 1 decreased in the miR-206-3p inhibition group. Furthermore, the myogenin and myosin heavy chain expression levels decreased in the miR-206-3p inhibition group (Fig. 4D-G).

miR-206-3p regulates osteogenic and myogenic differentiation via the classical β-catenin signaling pathway. As SFRP1 is the main antagonist of β-catenin signaling, the expression of GSK-3β, p-GSK-3β, β-catenin and nuclear β-catenin was detected after transfecting the BMSC and L6 cells. Compared with the control group, the protein levels of p-GSK-3β and β-catenin were lower (Fig. 5A-D) and nuclear β-catenin was significantly down-regulated (Fig. 5I and J) during the differentiation process in the miR-206-3p inhibition group. During the myogenesis of L6 cells, the expression levels of p-GSK-3β, β-catenin (Fig. 5E-H) and nuclear β-catenin decreased in the miR-206-3p inhibition group (Fig. 5K-L). There was no difference in the expression of GSK-3β between the inhibition and control groups.

Discussion

miR-206-3p is expressed in a number of cells, such as skeletal muscle cells, heart cells mesenchymal stem cells and brown adipocytes, but not in white adipocytes (24,25). A study in tumor cells proved the specific expression of miR-206-3p and inhibit cell migration and invasion in various cancers (26). Bone mineral density is regulated by osteoclasts and osteoblasts in the bone microenvironment within the basic multicellular unit, as well as osteocytes, bone lining cells, osteoma cells and vascular endothelial cells (27). For example, miR-206-3p promotes osteogenic differentiation by negatively regulating BMP3 expression in osteoblasts and can be transferred to osteoclasts to inhibit osteoclast bone resorption (28,29). Previous studies have found that a number of miRNAs have multiple roles in bone diseases; miRNAs play important regulatory roles in bone formation, bone healing and osteoblastogenesis and can regulate osteoclastogenesis or enter them to regulate cell functions (30,31).

Mechanical and chemical crosstalk exist between muscles and bones (32). Furthermore, some biochemical pathways, such as Dickkopf-1 and IL-6, affect both muscle and bone (32,33). The present study demonstrated that miR-206-3p affected muscle and bone differentiation by targeting SFRP1 and acting via the Wnt/β-catenin signaling pathway.

The present study performed transcriptome sequencing of the BMSCs in both groups, which revealed that SFRP1 was markedly elevated in the osteoporosis group. The SFRP gene family has five members (SFRP1-SFRP5) in the human and mouse genomes and it plays an important role in the development of cancer and inflammatory diseases (34). SFRP1 is involved in bone metabolism and homeostasis. For example, overexpression of SFRP1 in osteoblasts inhibits the parathyroid hormone-induced bone formation as well as the differentiation and maturation of osteoblasts (35). Simultaneously, SFRP1 plays a role in muscle proliferation and differentiation. For example, the addition of recombinant Sfrp1 to C2C12 or satellite cells inhibits muscle duct formation (36). Therefore, identifying the regulatory factors of the upstream and downstream pathways of SFRP1 may help determine the therapeutic targets of osteosarcopenia.

The present study hypothesized that miR-206-3p may bind to SFRP1 and found that SFRP1 and miR-206-3p were negatively associated in the BMSCs of the OVX and Sham groups. Subsequently, a DLR assay and transfection experiment indicated that miR-206-3p may directly target SFRP1 and affect the osteogenic differentiation of BMSC. This indicated that SFRP1 plays an important role in the occurrence and development of osteoporosis. These findings are consistent with a previous study in which miR-206-3p was demonstrated as a positive regulator of muscle differentiation and SFRP1 has inhibited myoblast differentiation (37). The present study further demonstrated that miR-206-3p affected the Wnt pathway by negatively regulating SFRP1, which promoted the myogenic differentiation of L6 cells.

The SFRPs family includes Wnt signaling antagonists that play a role in various diseases by regulating Wnt signaling (38). SFRP1 antagonizes Wnt signaling by competitively binding to the cysteine-rich Wnt receptor frizzled (39). The Wnt/β-catenin signaling pathway is closely associated with bone and muscle (40). The Wnt/β-catenin signaling pathway can regulate bone formation and absorption, muscle fiber formation and the activation of adult muscle stem cells (41-43). The typical Wnt/β-catenin signaling pathway inhibits the expression of GSK3β in BMSCs via the low density lipoprotein receptor-related protein co-receptor and it can promote the nuclear translocation of β-catenin in the cytoplasm. An increase in the β-catenin-T-cell factor (TCF) 4/lymphoid enhancer factor-1 (LEF1) complex in the nucleus activates the transcription of downstream osteogenic genes (44). In skeletal muscle, activation of Wnt signaling leads to an increase in the nuclear translocation of β-catenin. This in turn increases the interaction of β-catenin with TCF/LEF1 transcription factors, which promotes the expression of myogenesis-related target genes (45). The present study found that the protein levels of p-GSK-3β and nuclear β-catenin were significantly decreased in BMSCs treated with the miR-206-3p inhibitor. However, in L6 cells treated with the miR-206-3p inhibitor, the protein levels of p-GSK-3β and nuclear β-catenin were significantly decreased. These findings indicate that miR-206-3p promotes β-catenin signaling by negatively regulating SFRP1, which affects bone and muscle differentiation. This result is consistent with a previous study (40).

The present study found that mir-206-3p and SFRP1 has indeed been reported in the literature, but it was the first time to study and report the regulatory relationship between mir-206-3p, SFRP1 and β-catenin in osteoporosis and sarcopenia at the same time. The present study has several limitations. First, it only focused on SFRP1 and its upstream target, miR-206-3p,

after obtaining multiple differential genes via transcriptome sequencing. However, miR-206-3p may simultaneously affect other target genes and SFRP1 may be regulated by other miRNAs. Thus, a comprehensive study on the biological functions of miR-206-3p and SFRP may provide a deeper understanding of the development of diseases. Second, the present study used rat BMSCs and the verified myoblasts L6 cells, which do not fully represent the processes of bone and muscle formation in humans. Third, rats in the osteoporosis model group were ovariectomized to mimic postmenopausal osteoporosis in humans. The present study results need to be verified in studies with larger samples of human patients with osteoporosis. Mouse models of accelerated aging have been shown to be important animal models for studying musculoskeletal aging and related disorders (46,47). In the future, studies will model animals in osteosarcopenia and continue to explore the regulatory pathways of miR-206-3p and SFRP1 genes in osteosarcopenia.

In conclusion, miR-206-3p affects the Wnt/β-catenin signaling pathway by functionally targeting SFRP1. This in turn regulates bone and muscle differentiation. Therefore, miR-206-3p and SFRP1 may be novel targets for the treatment of osteosarcopenia.

Acknowledgements

Not applicable.

Funding

The present study was funded by the National Natural Science Foundation of China (grant no. 82172442), the Yunnan Provincial Department of Science and Technology Social Development Special Project (grant no. 202403AC100003), Major Science and Technology Special Project of Yunnan Provincial Science and Technology Program (grant no. 202102AA310042) and Opening Subjects of Clinical Medical Research Center of the First People's Hospital of Yunnan Province (grant no. 2022YJZX-GK17).

Availability of data and materials

The data generated in the present study are included in the figures and/or tables of this article.

Authors' contributions

CY and ZL jointly conceptualized this study, designed and conducted experiments and wrote and edited the manuscript. DY conceived this study, designed and conducted experiments and edited the manuscript. YL wrote the manuscript and contributed to the analysis and interpretation of the data. JF and YZ designed and implemented the experiment, and wrote the manuscript. ZP and SL made critical revisions to the manuscript. CY and SL confirm the authenticity of all raw data. All authors have read and approved the final manuscript.

Ethics approval and consent to participate

The experimental animal study protocol was approved by the Animal Care and Use Committee of the Kunming Medical University, Kunming, China (approval no. kmmu20230916). All animal experiments and handling were performed in accordance with the Guide for the Care and Use of Laboratory Animals published by the National Institutes of Health (NIH Publication No. 8523, revised 1985) (22).

Patient consent for publication

Not applicable.

Competing interests

The authors declare that they have no competing interests.

References

1. Kirk B, Zanker J and Duque G: Osteosarcopenia: Epidemiology, diagnosis and treatment-facts and numbers. J Cachexia Sarcopenia Muscle 11: 609-618, 2020.
2. Li GH, Cheung CL, Tan KC, Kung AW, Kwok TC, Lau WC, Wong JS, Hsu WWQ, Fang C and Wong IC: Development and validation of sex-specific hip fracture prediction models using electronic health records: a retrospective, population-based cohort study. EClinicalMedicine 58: 101876, 2023.
3. Yuan S and Larsson SC: Epidemiology of sarcopenia: Prevalence, risk factors and consequences. Metabolism 144, 155533, 2023.
4. Shimada H, Suzuki T, Doi T, Lee S, Nakakubo S, Makino K and Arai H: Impact of osteosarcopenia on disability and mortality among Japanese older adults. J Cachexia Sarcopenia Muscle 14: 1107-1116, 2023.
5. Locquet M, Beaudart C, Reginster JY and Bruyère O: Association between the decline in muscle health and the decline in bone health in older individuals from the SarcoPhAge cohort. Calcif Tissue Int 104: 273-284, 2019.
6. Clynes MA, Gregson CL, Bruyère O, Cooper C and Dennison EM: Osteosarcopenia: where osteoporosis and sarcopenia collide. Rheumatology (Oxford) 60: 529-537, 2021.
7. Inoue T, Maeda K, Nagano A, Shimizu A, Ueshima J, Murotani K, Sato K, Hotta K, Morishita S and Tsubaki A: Related factors and clinical outcomes of osteosarcopenia: A narrative review. Nutrients 13: 291, 2021.
8. Prockop DJ: Marrow stromal cells as stem cells for nonhematopoietic tissues. Science 276: 71-74, 1997.
9. Loh KM, Chen A, Koh PW, Deng TZ, Sinha R, Tsai JM, Barkal AA, Shen KY, Jain R, Morganti RM, *et al*: Mapping the pairwise choices leading from pluripotency to human bone, heart and other mesoderm cell types. Cell 166: 451-467, 2016.
10. Yin L, Yang Z, Wu Y, Denslin V, Yu CC, Tee CA, Lim CT, Han J and Lee EH: Label-free separation of mesenchymal stem cell subpopulations with distinct differentiation potencies and paracrine effects. Biomaterials 240: 119881, 2020.
11. Feng Z, Jin M, Liang J, Kang J, Yang H, Guo S and Sun X: Insight into the effect of biomaterials on osteogenic differentiation of mesenchymal stem cells: A review from a mitochondrial perspective. Acta Biomater 164: 1-14, 2023.
12. Shivdasani RA: MicroRNAs: Regulators of gene expression and cell differentiation. Blood 108: 3646-3653, 2006.
13. Wang E: MicroRNA, the putative molecular control for mid-life decline. Ageing Res Rev 6: 1-11, 2007.
14. Sun Y, Kuek V, Liu Y, Tickner J, Yuan Y, Chen L, Zeng Z, Shao M, He W and Xu J: MiR-214 is an important regulator of the musculoskeletal metabolism and disease. J Cell Physiol 234: 231-245, 2018.
15. Fariyike B, Singleton Q, Hunter M, Hill WD, Isales CM, Hamrick MW and Fulzele S: Role of MicroRNA-141 in the aging musculoskeletal system: A current overview. Mech Ageing Dev 178: 9-15, 2019.
16. Shang Q, Shen G, Chen G, Zhang Z, Yu X, Zhao W, Zhang P, Chen H, Tang K, Yu F, *et al*: The emerging role of miR-128 in musculoskeletal diseases. J Cell Physiol 236: 4231-4243, 2021.
17. Sun D, Chen Y, Liu X, Huang G, Cheng G, Yu C and Fang J: miR-34a-5p facilitates osteogenic differentiation of bone marrow mesenchymal stem cells and modulates bone metabolism by targeting HDAC1 and promoting ER-α transcription. Connect Tissue Res 64: 126-138, 2023.

18. Wang C, Zhu M, Yang D, Hu X, Wen X and Liu A: MiR-29a-3p inhibits proliferation and osteogenic differentiation of human bone marrow mesenchymal stem cells via targeting FOXO3 and repressing Wnt/β-catenin signaling in steroid-associated osteonecrosis. Int J Stem Cells 15: 324-333, 2022.
19. Wang YC, Yao X, Ma M, Zhang H, Wang H, Zhao L, Liu S, Sun C, Li P, Wu Y, *et al*: miR-130b inhibits proliferation and promotes differentiation in myocytes via targeting Sp1. J Mol Cell Biol 13: 422-432, 2021.
20. Yang L, Qi Q, Wang J, Song C, Wang Y, Chen X, Chen H, Zhang C, Hu L and Fang X: MiR-452 regulates C2C12 myoblast proliferation and differentiation *via* targeting *ANGPT1*. Front Genet 12: 640807, 2021.
21. van Rooij E, Liu N and Olson EN: MicroRNAs flex their muscles. Trends Genet 24: 159-166, 2008.
22. U.S. Office of Science and Technology Policy: Laboratory animal welfare; U.S. government principles for the utilization and care of vertebrate animals used in testing, research and training; notice. Fed Regist 50: 20864-20865, 1985.
23. Livak KJ and Schmittgen TD: Analysis of relative gene expression data using real-time quantitative PCR and the 2(-Delta Delta C(T)) method. Methods 25: 402-408, 2001.
24. Townley-Tilson WH, Callis TE and Wang D: MicroRNAs 1, 133 and 206: critical factors of skeletal and cardiac muscle development, function and disease. Int J Biochem Cell Biol 42: 1252-1255, 2010.
25. Walden TB, Timmons JA, Keller P, Nedergaard J and Cannon B: Distinct expression of muscle-specific microRNAs (myomirs) in brown adipocytes. J Cell Physiol 218: 444-449, 2009.
26. Wu K, Li J, Qi Y, Zhang C, Zhu D, Liu D and Zhao S: SNHG14 confers gefitinib resistance in non-small cell lung cancer by up-regulating ABCB1 via sponging miR-206-3p. Biomed Pharmacother 116: 108995, 2019.
27. Kular J, Tickner J, Chim SM and Xu J: An overview of the regulation of bone remodelling at the cellular level. Clin Biochem 45: 863-873, 2012.
28. Guo S, Gu J, Ma J, Xu R, Wu Q, Meng L, Liu H, Li L and Xu Y: GATA4-driven miR-206-3p signatures control orofacial bone development by regulating osteogenic and osteoclastic activity. Theranostics 11: 8379-8395, 2021.
29. Wang B, Yu P, Li T, Bian Y and Weng X: MicroRNA expression in bone marrow mesenchymal stem cells from mice with steroid-induced osteonecrosis of the femoral head. Mol Med Rep 12: 7447-7454, 2015.
30. Li H, Zhai Z, Qu X, Xu J, Qin A and Dai K: MicroRNAs as potential targets for treatment of osteoclast-related diseases. Curr Drug Targets 19: 422-431, 2018.
31. Li D, Liu J, Guo B, Liang C, Dang L, Lu C, He X, Cheung HY, Xu L, Lu C, *et al*: Osteoclast-derived exosomal miR-214-3p inhibits osteoblastic bone formation. Nat Commun 7: 10872, 2016.
32. Tagliaferri C, Wittrant Y, Davicco MJ, Walrand S and Coxam V: Muscle and bone, two interconnected tissues. Ageing Res Rev 21: 55-70, 2015.
33. Bakker AD and Jaspers RT: IL-6 and IGF-1 signaling within and between muscle and bone: How important is the mTOR pathway for bone metabolism? Curr Osteoporos Rep 13: 131-139, 2015.
34. van Loon K, Huijbers EJM and Griffioen AW: Secreted frizzled-related protein 2: A key player in noncanonical Wnt signaling and tumor angiogenesis. Cancer Metastasis Rev 40: 191-203, 2021.
35. Bodine PVN, Seestaller-Wehr L, Kharode YP, Bex FJ and Komm BS: Bone anabolic effects of parathyroid hormone are blunted by deletion of the Wnt antagonist secreted frizzled-related protein-1. J Cell Physiol 210: 352-357, 2007.
36. Descamps S, Arzouk H, Bacou F, Bernardi H, Fedon Y, Gay S, Reyne Y, Rossano B and Levin J: Inhibition of myoblast differentiation by Sfrp1 and Sfrp2. Cell Tissue Res 332: 299-306, 2008.
37. Yang Y, Sun W, Wang R, Lei C, Zhou R, Tang Z and Li K: Wnt antagonist, secreted frizzled-related protein 1, is involved in prenatal skeletal muscle development and is a target of miRNA-1/206 in pigs. BMC Mol Biol 16: 4, 2015.
38. Jiang P, Wei K, Chang C, Zhao J, Zhang R, Xu L, Jin Y, Xu L, Shi Y, Guo S, *et al*: SFRP1 negatively modulates pyroptosis of fibroblast-like synoviocytes in rheumatoid arthritis: A review. front immunol 13: 903475, 2022.
39. Bodine PVN and Komm BS: Wnt signaling and osteoblastogenesis. Rev Endocr Metab Disord 7: 33-39, 2006.
40. Yang YJ and Kim DJ: An overview of the molecular mechanisms contributing to musculoskeletal disorders in chronic liver disease: Osteoporosis, sarcopenia and osteoporotic sarcopenia. Int J Mol Sci 22: 2604, 2021.
41. Cossu G and Borello U: Wnt signaling and the activation of myogenesis in mammals. EMBO J 18: 6867-6872, 1999.
42. Hoeppner LH, Secreto FJ and Westendorf JJ: Wnt signaling as a therapeutic target for bone diseases. Expert Opin Ther Targets 13: 485-496, 2009.
43. Boudin E, Fijalkowski I, Piters E and Van Hul W: The role of extracellular modulators of canonical Wnt signaling in bone metabolism and diseases. Semin Arthritis Rheum 43: 220-240, 2013.
44. Law SM and Zheng JJ: Premise and peril of Wnt signaling activation through GSK-3β inhibition. iScience 25: 104159, 2022.
45. Shevtsov SP, Haq S and Force T: Activation of beta-catenin signaling pathways by classical G-protein-coupled receptors: Mechanisms and consequences in cycling and non-cycling cells. Cell Cycle 5: 2295-2300, 2006.
46. Yılmaz D, Mathavan N, Wehrle E, Kuhn GA and Müller R: Mouse models of accelerated aging in musculoskeletal research for assessing frailty, sarcopenia and osteoporosis-A review. Ageing Res Rev 93: 102118, 2024.
47. Zhang N, Chow SKH, Leung KS, Lee HH and Cheung WH: An animal model of co-existing sarcopenia and osteoporotic fracture in senescence accelerated mouse prone 8 (SAMP8). Exp Gerontol 97: 1-8, 2017.